Solid State Sciences 11 (2009) 676–682

Contents lists available at ScienceDirect

Solid State Sciences

journal homepage: www.elsevier.com/locate/ssscie

Mechanochemical synthesis of AlF_3 with NH_4F as fluorinating agent – Does it work?

G. Scholz*, E. Kemnitz

Humboldt-Universität zu Berlin, Institut für Chemie, Brook – Taylor – Str. 2, D – 12489 Berlin, Germany

ARTICLE INFO

Article history:
Received 12 September 2008
Received in revised form
14 October 2008
Accepted 28 October 2008
Available online 5 November 2008

Keywords:
Mechanochemistry
AlF_3
$(NH_4)_3AlF_6$

ABSTRACT

Followed by X-ray diffraction, MAS NMR and elemental analysis the mechanochemical reaction between $Al(OiPr)_3$, γ-AlOOH and $Al(ac)_2OH$ as possible aluminium sources on the one side, and NH_4F as fluorinating agent on the other side was studied. Encouraged by the successful mechanochemical synthesis of CaF_2 using the same fluorinating agent, the formation of AlF_3 was expected. However, it can be established that as long as NH_4F is supplied the formation of crystalline $(NH_4)_3AlF_6$ is observed instead.

1. Introduction

The application of mechanosynthesis on solid fluorides is very scarce in the literature until now. Few papers published so far are addressed to the mechanochemical synthesis of $AZnF_3$ compounds (A: K, Na, NH_4) with perovskite structures [1], the synthesis of complex fluorides ARF_4 (A: Li, Na, K; R: rare earth elements) [2], as well as the mechanochemical synthesis of lanthanum oxofluoride LaOF using LaF_3 and La_2O_3 [3]. Further milling studies on fluorides were focused on changes of fluorine ion conductivity [4–6], the influence of fluorine on phase transitions [7] or electrochemical activity [8].

Recently, one of us published results on mechanochemical reactions of NaF with AlF_3 [9]. It could be demonstrated that dependent on the molar ratio of the educts cryolite (Na_3AlF_6) and/or chiolite ($Na_5Al_3F_{14}$) is obtained as reaction products. These reactions do not proceed stoichiometrically yielding mixtures of at least two components: $Na_5Al_3F_{14}$ and AlF_3, or $Na_5Al_3F_{14}$ and Na_3AlF_6. Moreover, the state of order of the educts, and especially the access of humidity has a strong influence on the composition of the product mixture [10]. In addition, applying the molar ratio Na:Al = 1:1 and using NaF and β-$AlF_3 \cdot 3H_2O$ as educts, after several hours of milling surprisingly the thermodynamically unstable phase $NaAlF_4 \cdot H_2O$ was formed. The water content, either delivered from the educts or controlled by the gaseous atmosphere, plays a crucial role for the reactions investigated [10]. Additionally it was shown [11] that the mechanosynthesis does not only work for complex fluorides but also, as a first attempt, for the binary fluoride CaF_2. Using ammonium fluoride as fluorinating agent the simple mechanochemical reaction with calcium carbonate led to CaF_2 according to Eq. (1):

$$CaCO_3 + 2NH_4F \rightarrow CaF_2 + 2NH_3 + CO_2 + H_2O \quad (1)$$

Except CaF_2, all other products are volatile resulting in a nanocrystalline CaF_2 powder comparable to that of a separately milled one [11].

Therefore, it is the aim of the present work to follow the route of mechanosynthesis proposed for CaF_2 in a comparable way for aluminium fluoride, AlF_3. Different crystalline phases of AlF_3 are well known and characterized [12–20]. Strongly disordered aluminium fluoride prepared on a sol-gel fluorination synthesis route [21,22], so-called high-surface AlF_3 (HS-AlF_3), is meanwhile well-known as a strong Lewis acid catalyst for halogen exchange reactions [23]. So it would be of importance to find an alternative possibility making AlF_3 avoiding the up to now used wet chemical strategies. In addition it can be expected to obtain a catalytically active AlF_3 as product of mechanosynthesis as it was shown for the milling of pure crystalline α-AlF_3 [24].

To proceed successfully, the educts of the mechanochemical reaction have to be chosen in such a way that the anion of the aluminium compound and the cation of the fluorine educt are preferably volatile. To fulfill these conditions, in the present study NH_4F was used as in [11] as fluorinating agent, which can release NH_3. As aluminium source, aluminium isopropoxide $Al(OiPr)_3$, also used as precursor compound for the sol-gel fluorination [23] was

* Corresponding author. Tel.: +49 30 2093 7112.
E-mail address: gudrun.scholz@rz.hu-berlin.de (G. Scholz).

1293-2558/$ – see front matter © 2008 Elsevier Masson SAS. All rights reserved.
doi:10.1016/j.solidstatesciences.2008.10.011

used as educt. In principle, the following hypothetical reaction can be formulated in analogy to Eq. (1):

$$Al(OiPr)_3 + 3NH_4F \rightarrow AlF_3 + 3NH_3\uparrow + 3iPrOH\uparrow \quad (2)$$

The choice of other fluorinating agents like NaF, KF, or e.g. KHF_2 is not promising since the formation of sodium or potassium cryolites can be expected. On the other hand, beside $Al(OiPr)_3$ both γ-AlOOH and $Al(CH_3COO)_2OH$ were tested as possible reaction partners for the fluorination by NH_4F. In these cases the release of water or acetic acid, can be assumed at milling. Different molar ratios Al:F were selected ranging from 1:0.2 up to 1:6. In addition, milling experiments were guided separately for the aluminium educts to estimate structural consequences of the mechanical impact. Changes of the educts and the product formation were followed by X-ray powder diffraction and ^{27}Al and ^{19}F MAS NMR supported by elemental analysis.

2. Experimental

2.1. Preparation

Samples were milled in a commercial planetary mill "Pulverisette 7" (Fritsch, Germany) under access of air applying milling times of 4 h and 8 h. Each syalon vial was used with five syalon balls (m_{balls}: 14.8 g; m_{sample}: 2 g) and a rotational speed of 600 rpm. Milling under inert conditions was carried out by handling the vials in the glove box and using screw clamps for the transport. Only commercially available educts were used: $Al(OiPr)_3$ (Aldrich), γ-AlOOH (Nabaltec), $Al(CH_3COO)_2OH$ (Fluka), NH_4F (98%, Aldrich).

2.2. Elemental analysis

The elemental analysis of the samples was performed with a LECO CHNS-932 combustion equipment (C, H, N).

2.3. XRD

XRD measurements were performed using the FPM 7 equipment (Rich. Seiffert & Co., Freiberg) with Cu Kα radiation (Cu $K\alpha_{1,2}$, $\lambda = 1.5418$ Å; 2Θ range: $5° \leq 2\Theta \leq 64°$; step scan: 0.05°, step time: 5 s). Phases were identified by comparison with the ICSD powder diffraction file [25].

2.4. MAS NMR

^{19}F and ^{27}Al MAS NMR spectra were recorded on a Bruker AVANCE 400 spectrometer (Larmor frequencies: $\nu_{^{19}F} = 376.4$ MHz; $\nu_{^{27}Al} = 104.3$ MHz) using a 2.5 mm double-bearing magic angle spinning (MAS) probe (Bruker Biospin) and applying a spinning speed of 25 kHz if not otherwise indicated.

^{19}F MAS NMR ($I = 1/2$) spectra were recorded with a π/2 pulse duration of $p1 = 2$ μs, a spectrum width of 400 kHz, a recycle delay of 10 s and an accumulation number of 32. The isotropic chemical shifts δ_{iso} of ^{19}F resonances are given below with respect to the $CFCl_3$ standard. Existent background signals of ^{19}F could be completely suppressed with the application of a phase-cycled depth pulse sequence according to Cory and Ritchey [26].

^{27}Al MAS NMR ($I = 5/2$) spectra were recorded with an excitation pulse duration of 1 μs. A 1 M aqueous solution of $AlCl_3$ was used as reference for the chemical shift of ^{27}Al. The radio frequency magnetic field strength was taken as 58 kHz in frequency units ($t_{\pi/2} = 4.3$ μs in $AlCl_3$ solution). The recycle delay was chosen as 1 s. ^{27}Al spectra were simulated using dmfit2007 [27].

Table 1
^{19}F and ^{27}Al isotropic chemical shift values of educts and expected milling products.

Sample	$\delta_{i^{27}Al}$ [ppm]	$\delta_{i^{19}F}$ [ppm]
$Al(OiPr)_3$[a]	1.7 (AlO_6)	–
	61.5 (AlO_4)	–
AlOOH[b]	10.0 (AlO_6)	
NH_4F	–	−84.6
AlF_3 [c]	−16.0 (AlF_6)	−172.5
$(NH_4)_3AlF_6$	−0.7 (AlF_6)	−140.4

[a] Refs. [28,29].
[b] Ref. [36].
[c] Refs. [9,37].

3. Results

XRD and MAS NMR measurements are well suitable to distinguish between educts and expected products. All reflections and central NMR transitions are clearly separated from each other and allow an unambiguous assignment. The isotropic chemical shift values of educts and possible products are summed up in Table 1. Due to previously made experiences with milling of fluorides [9,11,24] serious structural consequences of the mechanical impact can already be expected for the educts. Therefore, these changes are presented separately.

3.1. Separate milling of the educts

As already be seen by the results of elemental analysis (see Table 2), milling has serious consequences for aluminium isopropoxide. Here, the carbon content decreases from 52.3% in the educt to 39.6% after milling, which corresponds to a sum formula of $Al(OiPr)_{1.5}(OH)_{1.5}$. On the other hand changes are negligible for NH_4F (see Table 2). The XRD powder patterns of crystalline $Al(OiPr)_3$ and γ-AlOOH recorded before and after milling are given in Fig. 1. For both Al compounds the milling effect is significant. $Al(OiPr)_3$ is completely amorphous after milling for 4 h. For γ-AlOOH the most intense reflections are still visible but with distinctly decreased amplitudes. This issue is again reinforced

Table 2
Results of elemental analysis of educts and milling products.

Sample	*C* [wt%]	*H* [wt%]	*N* [wt%]
$Al(OiPr)_3$, theory	52.9	10.3	
$Al(OiPr)_3$, educt	52.3	10.1	
$Al(OiPr)_3$, milled	39.6	8.2	
NH_4F, theory	–	10.8	37.8
NH_4F, educt	–	10.2	38.0
NH_4F, milled	–	10.0	38.0
$(NH_4)_3AlF_6$, theory	–	6.2	21.5
Milling products			
Milling of $Al(OiPr)_3$ with NH_4F:			
Molar ratio (Al:F)			
1:0.2	37.5	7.2	0.5
1:0.5	36.4	7.4	1.4
1:1	34.5	7.9	3.6
1:3	3.0	5.0	13.1
1:6	–	5.8	21.2
1:1 (dry milling)	40.5	9.0	3.3
1:3 (dry milling)	16.3	6.7	12.2
Milling of AlOOH with NH_4F			
Molar ratio Al:F			
1:1	–	3.9	8.0
1:3	–	6.9	21.4
1:1 (AlOOH, 8 h[a])	–	3.0	6.5
1:3 (AlOOH, 8 h[a])	–	4.3	14.7

[a] AlOOH was pre-milled before milling the mixture with NH_4F.

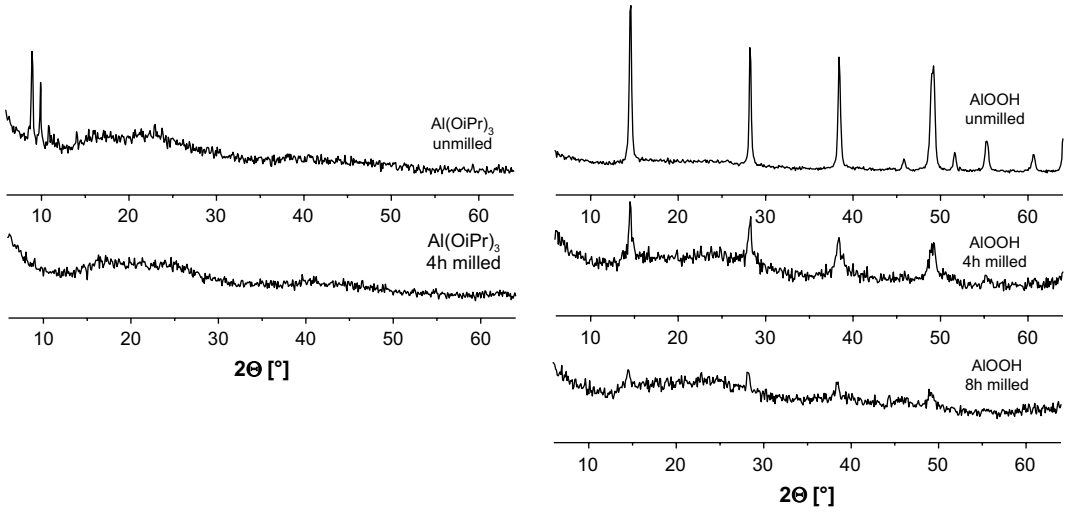

Fig. 1. X-ray powder diffractograms of unmilled and milled Al(O*i*Pr)$_3$ and AlOOH samples.

after 8 h of milling. Milling of aluminium acetate led to an amorphous product as well (not shown here).

^{27}Al MAS NMR spectra as given in Fig. 2 disclose strong local structural changes initiated by milling. Solid aluminium isopropoxide has a tetrameric structure with four- and six-fold oxygen coordinated aluminium sites [28,29]. The NMR parameters of these two sites were published in Refs. [28,29]. After milling, the original structure is destroyed and three aluminium signals with $\delta_{^{27}Al}$ at about 0 ppm, 30 ppm and 60 ppm appear. They are indicative for sixfold, fivefold and fourfold oxygen coordinated aluminium sites, respectively (see Fig. 2). Surprisingly, a similar pattern is obtained after milling of γ-AlOOH, changing the Al coordination from a sixfold one to six-, five- and four-fold coordinated sites as already observed by MacKenzie et al. [30].

The simulation of the ^{27}Al spectra was performed using Czjzek distribution functions for each species [31,32]. The respective deconvolutions of the spectra are included in Fig. 2. Parameters of the simulation are given in Table 3. Although it is not obvious on a first view from the experimental spectra (Fig. 2), the simulation including Czjzek distribution functions results in a comparable relative integral portion of AlO_6 sites for both milled samples. For γ-AlOOH, the mechanical impact leads first to an opening of the AlO_6 units exclusively present in the unmilled sample. AlO_5 species are formed and in a further step also AlO_4 with a smaller proportion (see Table 3). In contrast, in Al(O*i*Pr)$_3$ milling affects first mainly the AlO_4 units, already present in the matrix. This results in a decrease of their proportion from about 70% to 38% accompanied by the formation of AlO_5 and new AlO_6 units. These findings are supported

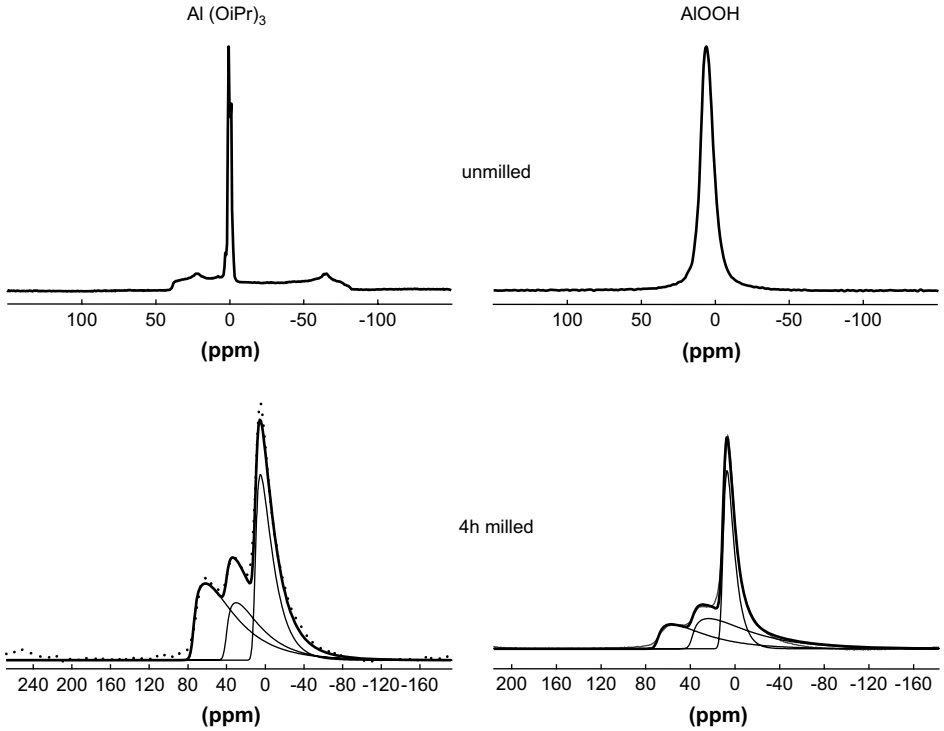

Fig. 2. ^{27}Al MAS NMR spectra (central lines) of unmilled and 4 h milled Al(O*i*Pr)$_3$ and AlOOH samples. Parameters for the deconvolution of the spectra are given in Table 3.

Table 3
^{27}Al NMR parameters of unmilled and milled Al(O*i*Pr)$_3$ and AlOOH samples.

Sample/parameter	δ_{iso} [ppm]	$\nu_{Q\eta}$[a] [kHz]
Al(O*i*Pr)$_3$		
Unmilled	1.7 (30% AlO_6)[b]	269[b]
	61.5 (70% AlO_4)	1871
4 h milled	11.3 (38% AlO_6)	700
	40.2 (24% AlO_5)	1000
	74.3 (38% AlO_4)	1100
AlOOH		
Unmilled	10.0 (100% AlO_6)	427[c]
4 h milled	11.0 (41% AlO_6)	500
	39.1 (35% AlO_5)	1200
	70.1 (24% AlO_4)	1100

[a] Quadrupolar product, taking into account both ν_Q and η: $\nu_{Q\eta} = \nu_Q\sqrt{1+\eta^2/3}$..
[b] Refs. [28,29].
[c] Ref. [36].

by ^{1}H–^{13}C CP MAS experiments (not shown here). The latter give clear indications for an attack of the mechanical impact on the outer O*i*Pr-groups of Al(O*i*Pr)$_3$ and a partial survival of bridging –CH and –CH_3 groups with chemical shift values between the terminal and bridging position.

After milling, both γ-AlOOH and Al(O*i*Pr)$_3$ contain highly reactive AlO_5 sites suitable for chemical reactions with fluorinating agents.

3.2. Milling of Al(OiPr)$_3$ with NH_4F

Milling of these two compounds was performed with six different Al:F molar ratios, ranging from 1:0.2 up to 1:6. Additionally, dry milling was performed for two mixtures with the molar ratios Al:F as 1:1 and 1:3. The lowest fluorine supply was chosen to follow first steps of fluorination, whereas the highest fluorine proportion should give an answer what happens in the case of fluorine excess.

Fig. 3 shows the ^{27}Al and ^{19}F MAS NMR spectra (central lines) for the three mixtures with the lowest fluorine content as well as an excess of fluorine. Fluorine NMR exhibits two signals: (i) a narrow one at −140 ppm, and (ii) a broader line with the maximum at about −155 ppm. The latter is more and more suppressed with increasing fluorine proportion.

The ^{27}Al spectrum of the 1:0.2 mixture reflects the overall features of milled Al(O*i*Pr)$_3$ superimposed by a new narrow line at ∼0 ppm along with new AlO_5 and AlO_4 species (see Fig. 2). With increasing fluorine supply the signal at 0 ppm is growing. This trend continues up to the highest proportion of fluorine with the result that finally only one Al signal at 0 ppm and one F signal at −140 ppm remain. In comparison with Table 1 it is clear that these signals do not origin from AlF_3, which was the expected product for this reaction. In fact, these are the typical signals of $(NH_4)_3AlF_6$ which is in agreement with XRD findings.

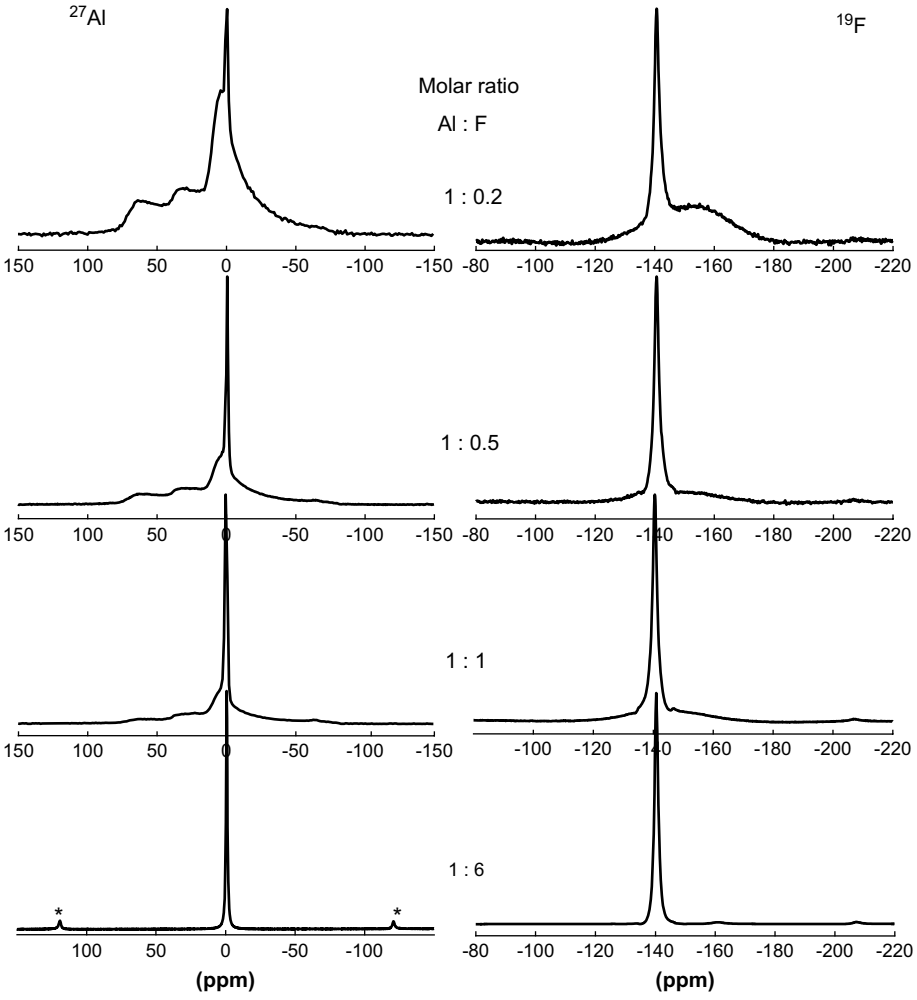

Fig. 3. ^{27}Al and ^{19}F MAS NMR spectra (central lines) of milled Al(O*i*Pr)$_3$–NH_4F mixtures applying different Al:F ratios as given in the Figure (*: spinning side bands for $\nu_{rot} = 12.5$ kHz).

Milling under dry conditions is less efficient than under air conditions as shown in Fig. 4. Under inert conditions the product mixture contains a higher content of non-transformed and less distorted crystalline $Al(OiPr)_3$ for each fluorine ratio (cf. Fig. 4, for comparison Fig. 2). Especially the fourfold oxygen coordinated aluminium sites with their large quadrupolar coupling constant [28,29] support this statement.

3.3. Milling of γ-AlOOH with NH_4F

X-ray diffractograms of milled mixtures of γ-AlOOH and NH_4F are given in Fig. 5. Using crystalline educts with an 1:1 composition, NH_4F is consumed during the milling process (Fig. 5a). Reflections of γ-AlOOH (*o*; PDF-Nr.: 83–2384) are still visible together with first reflections of $(NH_4)_3AlF_6$ (PDF number: 22–1036). Beginning the milling process with a mechanically activated pre-milled AlOOH sample (8 h milled; molar ratio of the educts 1:1), the milling process is much more efficient and the XRD pattern gives only the reflections of $(NH_4)_3AlF_6$ (*; Fig. 5b).

Using the 1:3 mixture of crystalline educts, the main NH_4F reflections (PDF-Nr.: 35–758) are still visible after 4 h milling (+; Fig. 5c). Additional reflections appear which can be attributed to $(NH_4)_3AlF_6$. Even in this case, the latter is much more pronounced

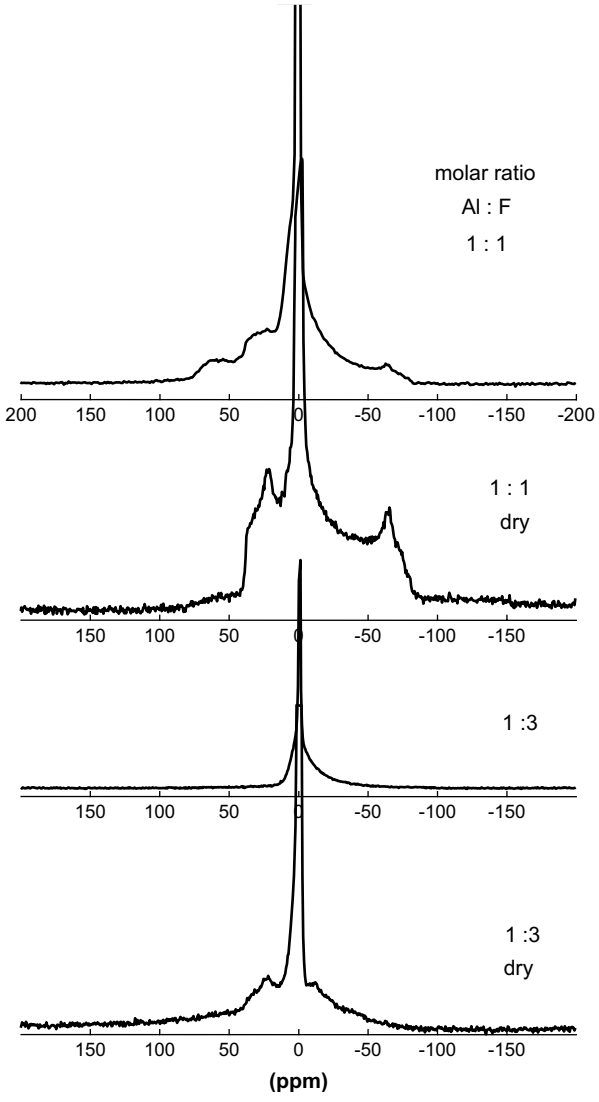

Fig. 4. Enlargement of the ^{27}Al MAS NMR spectra (central lines) of $Al(OiPr)_3$–NH_4F mixtures recorded after milling under ambient and dry conditions.

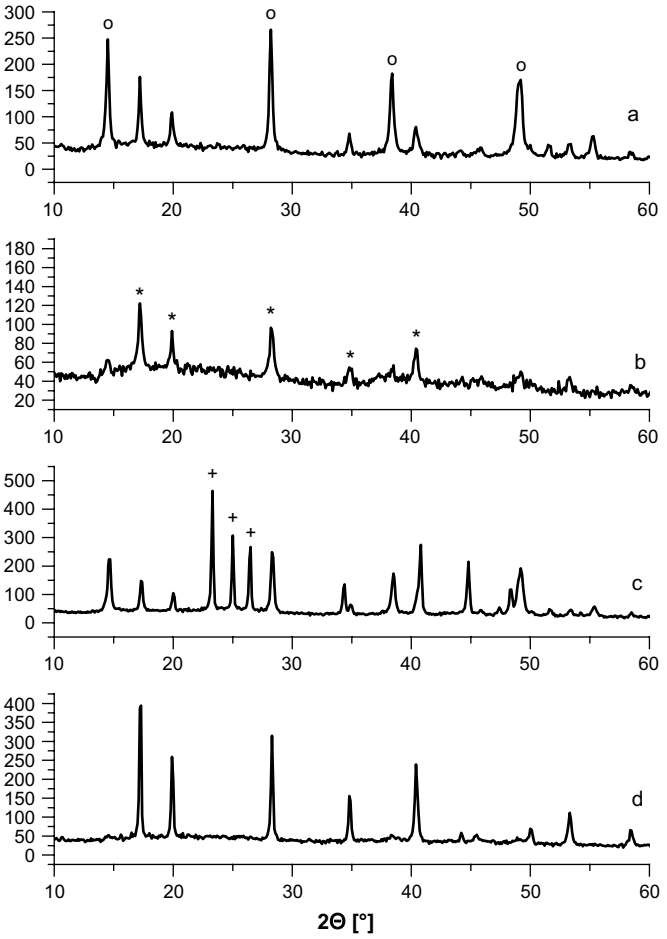

Fig. 5. X-ray powder diffractograms obtained after milling of: a) crystalline AlOOH with NH_4F, Al:F = 1:1; b) 8 h pre-milled AlOOH with NH_4F, Al:F = 1:1; c) crystalline AlOOH with NH_4F, Al:F = 1:3; d) 8 h pre-milled AlOOH with NH_4F, Al:F = 1:3; *o* reflections of AlOOH (PDF: 83–2384); * reflections of $(NH_4)_3AlF_6$ (PDF:22–1036); + reflections of NH_4F (PDF: 35–758).

starting with already pre-milled AlOOH samples. Now, for mixtures with both compositions only the reflections of $(NH_4)_3AlF_6$ remain (Fig. 5d).

Milling of $Al(CH_3COO)_2OH$ with NH_4F gives no new chemical results and is therefore not separately presented here. In agreement with the above findings the observed final species is $(NH_4)_3AlF_6$.

All XRD findings are supported by ^{27}Al and ^{29}F MAS NMR experiments. For a clear presentation the spectra shown in Fig. 6 are focused on the mixtures using the 8 h pre-milled γ-AlOOH sample. At the end, both solid state NMR and XRD indicate the formation of phase pure well crystalline $(NH_4)_3AlF_6$.

4. Discussion and conclusion

The above-presented results clearly indicate strong changes occurring at mechanical milling of the educts. Compact structures are broken as demonstrated for boehmite (γ-AlOOH) and aluminium isopropoxide ($Al(OiPr)_3$). The resulting mechanically activated AlO_4, AlO_5 and AlO_6 coordination polyhedra (cf. Fig. 2) are able to undergo chemical reactions with a fluorinating agent. Depending on the supplied fluorine amount a clear trend is visible with the formation of two *new* NMR signals, which are finally the only remaining signals with higher fluorine supply: (i) at ~0 ppm (^{27}Al) and (ii) at −140 ppm (^{19}F) (see Figs. 3 and 6).

However, in contradiction to the expected reaction ending up with AlF_3 (see Eq. (2)), the obviously energetically favored reaction

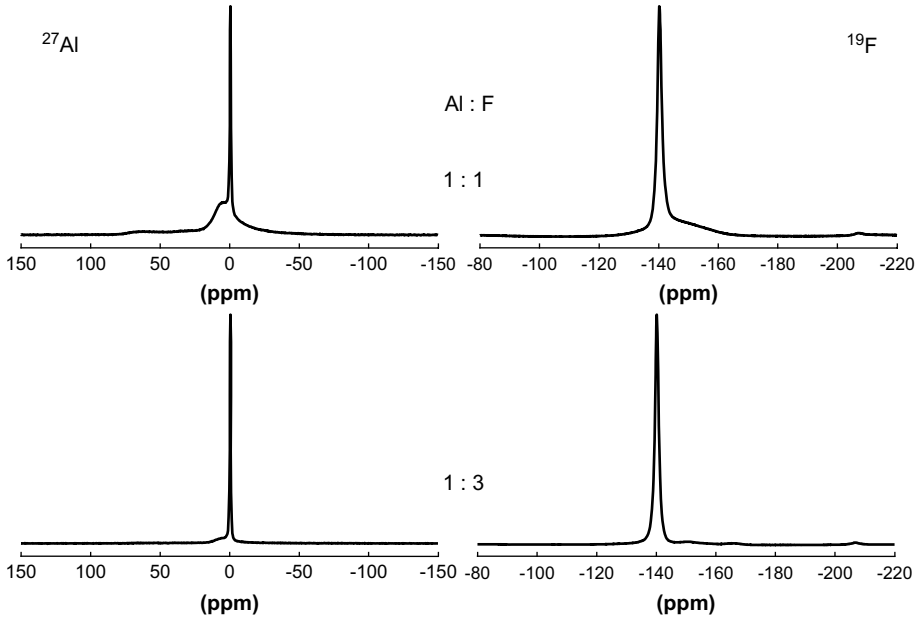

Fig. 6. ^{27}Al and ^{19}F MAS NMR spectra (central lines) of milled AlOOH–NH_4F mixtures applying two different Al:F ratios as given in the Figure. (The AlOOH sample was pre-milled for 8 h).

path results in the formation of $(NH_4)_3AlF_6$. A new, and unexpected equation can be written now for *all* reactions examined in this study:

$$Al(OiPr)_3 + 6NH_4F \rightarrow (NH_4)_3AlF_6 + 3NH_3 + 3iPrOH \quad (3)$$

The amount of ammonium hexafluoroaluminate strongly depends on the fluorine supply and the reaction (Eq. (3)) proceeds in the case of Al(O*i*Pr)$_3$ stoichiometrically with an Al:F ratio of 1:6 (see also Fig. 3). The latter is supported by the elemental analysis (Table 2) giving practically the theoretical N- and H-percentages of $(NH_4)_3AlF_6$ after milling the mentioned 1:6 mixture.

Changes in the product composition with fluorine supply are comparable using pre-milled AlOOH and NH_4F as educts instead. The use of crystalline boehmite γ-AlOOH as educt suggests a higher N content after milling (see Table 2, 1:3 mixture). However, in this case contributions from non-consumed NH_4F to the total amount of N still exist, as shown in Fig. 5.

From the experiments carried out in the present study it is clear now, that in contradiction to CaF_2 [11] the aspired formation of AlF_3 is not possible on the mechanochemical way followed here. Instead, another interesting and unexpected reaction takes place: the mechanochemical, and stoichiometrical formation of well crystalline $(NH_4)_3AlF_6$. Finally, starting from this compound, AlF_3 can be formed in a well-known subsequent reaction by thermal annealing up to 800 °C [33].

Surprisingly, the well-known path of AlF_3 formation by thermal decomposition of $AlF_3 \cdot 3H_2O$ [34] is *not* transferable to a mechanical treatment of the aluminium fluoride hydrates (not expl. shown here). The large mechanical impact initiates a deviating reaction channel ending up again with aluminium fluoride hydrates.

A formation of AlF_3 at milling is obviously hampered by the fluorination agent, which has to have a volatile cationic part. Even in the case of larger cations like $N(CH_3)_4F$ instead of NH_4F more complex reactions are observed which did not allow an assignment of the products so far. On the other hand a similar issue as in the present study was described in the literature for the formation of $(NH_4)_3GaF_6$, which can be initiated by milling of $GaF_3 \cdot 3H_2O$ with NH_4F [35]. For the formation of $(NH_4)_3AlF_6$ the last named reaction holds for the reaction of $AlF_3 \cdot 3H_2O$ with NH_4F as well (not shown here).

Acknowledgement

J. Kölsch is kindly acknowledged for several milling experiments, U. Kätel and Dr. A. Zehl for elemental ananlysis.

References

[1] J. Lee, Q. Zhang, F. Saito, Chem. Lett. (2001) 700.
[2] J. Lu, Q. Zhang, F. Saito, Chem. Lett. (2002) 1176.
[3] J. Lee, Q. Zhang, F. Saito, J. Am. Ceram. Soc. 84 (2001) 863.
[4] M. Kumar, S.S. Sekhon, J. Phys. D: Appl. Phys. 34 (2001) 2995.
[5] M. Kumar, K. Yamada, T. Okuda, S.S. Sekhon, Phys. Status Solidi (b) 239 (2003) 432.
[6] M. Uno, M. Onitsuka, Y. Ito, S. Yoshikado, Solid State Ionics 176 (2005) 2493.
[7] Y. Wu, Y. Zhang, G. Pezotti, J. Mater. Lett. 52 (2002) 366.
[8] M. Bervas, F. Badway, L.C. Klein, G.G. Amatucci, Electrochem. Solid State Lett. 8 (4) (2005) A179.
[9] G. Scholz, O. Korup, Solid State Sci. 8 (2006) 678.
[10] G. Scholz, M. Feist, E. Kemnitz, Solid State Sci. 10 (2008) 1640.
[11] G. Scholz, I. Dörfel, D. Heidemann, M. Feist, R. Stösser, J. Solid State Chem. 179 (2006) 1119.
[12] J. Ravez, A. Mogus-Milankovic, J.P. Chaminade, P. Hagenmuller, Mater. Res. Bull. 19 (1984) 1311.
[13] P. Daniel, A. Bulou, M. Rousseau, J. Nouet, J.L. Fourquet, M. Leblanc, R. Burriel, J. Phys.: Condens. Matter 2 (1990) 5663.
[14] A. Le Bail, C. Jacoboni, M. Leblanc, R. De Pape, H. Duroy, J.L. Fourquet, J. Solid State Chem. 77 (1988) 96.
[15] J.L. Fourquet, M. Riviere, A. Le Bail, M. Nygrens, J. Grins, Eur. J. Solid State Inorg. Chem. 25 (1988) 535.
[16] N. Herron, D.L. Thorn, R.L. Harlow, G.A. Jones, J.B. Parise, J.A. Fernandez-baca, T. Vogt, Chem. Mater. 7 (1995) 75.
[17] A. Le Bail, J.L. Fourquet, U. Bentrup, J. Solid State Chem. 100 (1992) 151.
[18] P. Daniel, A. Bulou, M. Rousseau, J. Nouet, Physiol. Rev. B42 (1990) 10545.
[19] G. Scholz, R. Stösser, J.Y. Buzaré, Ch Legein, G. Silly, Appl. Magn. Reson. 18 (2000) 199.
[20] T. Krahl, E. Kemnitz, J. Fluorine Chem. 127 (2006) 663.
[21] E. Kemnitz, U. Groß, S. Rüdiger, C.S. Shekar, Angew. Chem. Int. Ed. 42 (2003) 4251.
[22] S. Rüdiger, U. Groß, E. Kemnitz, J. Fluorine Chem. 128 (2007) 353.
[23] S. Rüdiger, G. Eltanany, U. Groß, E. Kemnitz, J. Sol-Gel. Sci. Technol. 41 (2007) 299.
[24] G. Scholz, R. König, J. Petersen, B. Angelow, I. Dörfel, E. Kemnitz, Chem. Mater. 20 (2008) 5406.
[25] JCPDS-ICCD-International Centre for Diffraction Data: PDF-2 Database, USA, Release 2001.
[26] D.G. Cory, W.M. Ritchey, J. Magn. Reson. 80 (1988) 128.
[27] D. Massiot, F. Fayon, M. Capron, I. King, S. Le Calve, B. Alonso, J.O. Durand, B. Bujoli, Z.H. Gan, G. Hoatson, Magn. Reson. Chem. 40 (2002) 70.
[28] A. Abraham, R. Prins, J.A. van Bokhoven, E.R.H. van Eck, A.P.M. Kentgens, J. Phys. Chem. B 110 (2006) 6553.

[29] R. König, Diploma Thesis, Humboldt University of Berlin, 2006.
[30] K.J.D. MacKenzie, J. Temuujin, M.E. Smith, P. Angerer, Y. Kameshima, Thermochim. Acta 359 (2000) 87.
[31] D. Neuville, L. Cormier, D. Massiot, Geochim. Cosmochim. Acta 68 (2004) 5071.
[32] J.B. d'Espinose de Lacaillerie, C. Fretigny, D. Massiot, J. Magn. Reson. 192 (2008) 244.
[33] L.K. Beck, B. Haendler-Kugler, H.M. Haendler, J. Solid State Chem. 8 (1973) 312.
[34] D.-H. Menz, A. Zacharias, L. Kolditz, J. Therm. Anal. 33 (1988) 811.
[35] J. Lu, Q. Zhang, J. Wang, F. Saito, J. Am. Ceram. Soc. 87 (2004) 1814.
[36] R. Stösser, G. Scholz, J.Y. Buzaré, G. Silly, M. Nofz, D. Schultze, J. Am. Ceram. Soc. 88 (10) (2005) 2913.
[37] G. Silly, Ch. Legein, J.Y. Buzaré, F. Calvayrac, Solid State Nucl. Res. 25 (2004) 241.